applied sciences

IMPACT FACTOR 2.5

CITESCORE 5.5

Article

Recoil Energy in Electron Capture Beta Decay and the Search for Sterile Neutrinos

Lorcan M. Folan, Philip Kazantsev and Vladimir I. Tsifrinovich

MDPI

https://doi.org/10.3390/app15179502

applied sciences

MDPI

Article

Recoil Energy in Electron Capture Beta Decay and the Search for Sterile Neutrinos

Lorcan M. Folan, Philip Kazantsev and Vladimir I. Tsifrinovich *

Department of Applied Physics, NYU Tandon School of Engineering, 2 MetroTech Center, Brooklyn, NY 11201, USA; folan@nyu.edu (L.M.F.); philkazantsev@gmail.com (P.K.)
* Correspondence: vtsifrin@nyu.edu; Tel.: +1-646-997-3473

Abstract

The left-handed electron neutrino generated in nuclear beta decays may be mixed with a hypothetical right-handed sterile neutrino with a mass much greater than the masses of the mass states of the active (electron, muon, and tau) neutrinos. In electron capture beta decay, the emitted neutrino may sometimes collapse into a sterile neutrino, reducing the recoil energy of the daughter atom. In this paper, we consider the electron capture beta decay of a ^{7}Be atom from the point of view of the possible detection of sterile neutrinos. We study theoretically the recoil energy of the daughter ^{7}Li atom. There are two decay channels for the ^{7}Be atoms: a direct decay to the nuclear ground state of the daughter atom with neutrino radiation and decay to the nuclear excited state of the daughter atom with neutrino radiation, followed by decay to the nuclear ground state with radiation of a γ-ray photon. For the first channel, the exact analytical expression for the recoil kinetic energy of the daughter atom is available in the literature. We derived exact analytical expressions for the recoil kinetic energy in the second decay channel. This recoil energy depends on the angle between the directions of motion of the neutrino and the photon. We point out that for a massless neutrino, the difference between the recoil energy in the first channel and the maximum recoil energy in the second channel is exactly zero. Thus, detection of a finite difference between the two energies would confirm the radiation of a massive neutrino. We also suggest another approach to the detection of massive neutrinos: the difference between the maximum and minimum recoil energies for the second channel changes significantly when a sterile neutrino is radiated. This effect could potentially be used for the detection of a sterile neutrino.

Keywords: electron neutrino; sterile neutrino; electron capture beta decay; recoil energy

Academic Editor: Richard Kouzes

Received: 2 August 2025
Revised: 22 August 2025
Accepted: 26 August 2025
Published: 29 August 2025

Citation: Folan, L.M.; Kazantsev, P.; Tsifrinovich, V.I. Recoil Energy in Electron Capture Beta Decay and the Search for Sterile Neutrinos. *Appl. Sci.* **2025**, *15*, 9502. https://doi.org/10.3390/app15179502

1. Introduction

Neutrinos and antineutrinos are the most elusive and mysterious elementary particles in contemporary physics. We begin our paper with a brief review of the properties of these particles. Neutrinos are always observed to have left-handed helicity (the spin angular momentum is directed opposite to the linear momentum), while antineutrinos always have right-handed helicity (the spin angular momentum is directed parallel to the linear momentum). The precise nature of the difference between a neutrino and an antineutrino is unresolved. A real distinction exists if the neutrino and the antineutrino are spin ½ "Dirac fermions." In this case, the neutrino and antineutrino are different particles, described by different quantum fields. However, these two particles may also be spin ½ "Majorana fermions," described by the same quantum field. In this case, neutrinos

and antineutrinos are the same particles with different helicities, analogous to left and right-circularly polarized photons.

There are three different flavors (i.e., types) of neutrinos and antineutrinos: electron, muon, and tau. The most abundant in the Universe are, probably, the relic neutrinos, which decoupled from the other fundamental particles about 1 s after the Big Bang. The relic neutrinos are expected to contain all three flavors in approximately equal proportion [1]. Currently, the energies of these relic neutrinos are insufficient for their direct detection. However, the relic neutrinos influence the spatial fluctuations of the cosmic microwave background, and this influence was detected [2].

Nuclear reactors generate large numbers of electron antineutrinos. The fission of heavy nuclei, e.g., ^{235}U, produces neutron-rich daughter nuclei, which undergo beta decay:

$$Z \rightarrow (Z+1) + e^- + \overline{\nu}_e. \quad (1)$$

Here, Z is the atomic number of the parent nucleus and e^- and $\overline{\nu}_e$ are the electron and the electron antineutrino. This reaction shows that, inside the nucleus, a neutron decays into a proton while radiating an electron and an electron antineutrino. On a more fundamental level, inside the neutron, a down quark (d) with negative electric charge $(-1/3)e$ transforms into an up quark (u) with positive charge $(2/3)e$ while radiating a W^- boson of charge $(-e)$. The W^- boson mediates the weak interaction. It decays by emitting an electron and an electron antineutrino. Due to such beta decays, about 4.5% of the fission energy released in nuclear reactors is radiated away as electron antineutrinos [3]. First observed in the 1950s, these antineutrinos are now detected routinely. The maximum energy of an antineutrino radiated by nuclear reactors is about 10 MeV. Radioactive isotopes present in the Earth, e.g., ^{238}U, also produce electron antineutrinos in beta decay processes [4].

Collisions between cosmic rays (typically protons) and atoms in the atmosphere generate atmospheric neutrinos and antineutrinos of both electron and muon flavors, with a wide range of energies up to at least 200 TeV [5]. The process of generation is the following. Byproducts of such collisions, e.g., positively charged pions, decay into positively charged antimuons μ^+ and muon neutrinos ν_μ:

$$\pi^+ \rightarrow \mu^+ + \nu_\mu. \quad (2)$$

A positively charged pion, or pi meson, has zero spin and consists of an up quark (u) of charge $(2/3)e$ and a down antiquark $\overline{d}$ of charge $(1/3)e$: $\pi^+ = u\overline{d}$. In the same way, a negatively charged antipion π^-, which consists of an up antiquark and a down quark, decays into a negatively charged muon μ^- and a muon antineutrino $\overline{\nu}_\mu$. A muon decays into an electron, a muon neutrino, and an electron antineutrino, while an antimuon decays into a positron (antielectron), an electron neutrino, and a muon antineutrino:

$$\mu^- \rightarrow e^- + \nu_\mu + \overline{\nu}_e,$$

$$\mu^+ \rightarrow e^+ + \overline{\nu}_\mu + \nu_e. \quad (3)$$

A typical particle accelerator may produce a beam of muon neutrinos and antineutrinos with energies in the range from MeV to GeV [6]. For example, if an accelerated proton beam hits a stationary target, positively charged pions π^+ are produced and can be separated from other particles. Then, the positively charged pions decay in flight into antimuons μ^+ and muon neutrinos, as shown in Formula (2). At the Large Hadron Collider (LHC), neutrinos and antineutrinos of all flavors with energies in the TeV region were detected in the ForwArd Search ExpeRiment (FASER) [7]. In the LHC, two counter-propagating beams of protons collide, producing other hadrons (particles composed of quarks and antiquarks)

which decay, producing neutrinos and antineutrinos, similar to the processes shown in Formulas (2) and (3).

The largest source of neutrinos near the Earth's surface is the core of the Sun [8]. The nuclear reaction generating the overwhelming majority of solar neutrinos is the fusion of two protons into a deuteron ^{2}H, which contains one proton and one neutron. This reaction generates a positron and an electron neutrino:

$$p^+ + p^+ \rightarrow {}^2H + e^+ + \nu_e. \quad (4)$$

The energy of the solar neutrinos produced by this reaction ("pp neutrinos") is relatively small (below 420 keV), but other nuclear reactions occurring in the core of the Sun produce neutrinos of energy up to 18 MeV [8]. Neutrinos and antineutrinos with energies below 100 MeV are also generated during the core collapse of massive stars [9]. In the process of the collapse, protons and electrons fuse, forming neutrons while radiating electron neutrinos. Also, the initial temperature of the collapsed core is very high (about 10^{11} K), and thermal energy is converted into neutrinos through pair production of neutrinos and antineutrinos of all flavors.

An intriguing property of the different neutrino flavors is that each flavor $|\nu_\alpha\rangle$, where α denotes a flavor (α = e, μ, τ), is a superposition of at least three "neutrino mass states," which for simplicity we denote as $|1\rangle$, $|2\rangle$, and $|3\rangle$. The mass states are the states with definite rest mass values, labeled m_1, m_2, and m_3. A major consequence of this property is the phenomenon of neutrino oscillations. During flight through free space, a neutrino of one flavor may transform into another flavor. For example, the muon neutrino produced in a pion decay may transform in flight into an electron or a tau neutrino. In order to understand neutrino oscillations, it is instructive to consider an analogy with electron spin precession.

Consider a neutral atom in an electronic ground S-state with a single unpaired electron (e.g., lithium) passing through a Stern-Gerlach apparatus, which measures the x-component of the atomic spin. After passing through the Stern-Gerlach apparatus, the electron spin of the atom points either in the positive or negative x-direction. We can call these two states the (+x) flavor ($|+\rangle$ state) and ($-$x) flavor ($|-\rangle$ state). Suppose that after passing through the Stern-Gerlach apparatus, the spin has the (+x) flavor. Let the atom then propagate through a region where a magnetic field points in the negative z-direction. (We choose the negative z-direction for the magnetic field because in the ground state, the electron spin points opposite to the magnetic field.) In the magnetic field, the "energy states" $|0\rangle$ and $|1\rangle$ have definite values of energy, corresponding to the (+z) and ($-$z) spin directions. The original spin flavor (+x) is then a superposition of the two energy states:

$$|+\rangle = 2^{-\frac{1}{2}}(|0\rangle + |1\rangle). \quad (5)$$

When the atom experiences the magnetic field, its spin state $|\psi\rangle$ must change because the flavor state $|+\rangle$ is not a stationary energy state:

$$|\psi\rangle = 2^{-\frac{1}{2}}\left\{\exp\left(\frac{i\omega t}{2}\right)\right\}|0\rangle + \exp\left\{\left(\frac{-i\omega t}{2}\right)\right\}|1\rangle = \cos\left(\frac{\omega t}{2}\right)|+\rangle + i * \sin\left(\frac{\omega t}{2}\right)|-\rangle. \quad (6)$$

Here, $\omega = \gamma_e B$ is the frequency of the Larmor precession, which is equal to the transition frequency between the electron spin states $|0\rangle$ and $|1\rangle$, γ_e is the electron gyromagnetic ratio, and B is the magnitude of the magnetic field. If one uses a second Stern-Gerlach device to measure the flavor of the spin at a distance (d) from the first apparatus, the probability to obtain the (+x) flavor will be $P+ = \cos^2(\omega d/2v)$, where v is the speed of the atom, and the time t in expression (6) equals d/v. Correspondingly, the probability

to observe the (−x) flavor $P- = \sin^2(\omega d/2v)$. The phase difference ωt between the two energy states increases with distance d, and the two probabilities oscillate. For example, with $\omega d/2v = \pi/4$, the probability to observe the (−x) spin flavor is $P- = P+ = ½$, and for, $\omega d/2v = \pi/2$, we have $P+ = 0$, $P- = 1$, i.e., the +x flavor changes to the −x flavor.

Just as happens in the case of an electron spin propagating in a magnetic field, when neutrinos propagate in free space, the phase differences between the mass states change, which is detectable as a change in the neutrino flavor. However, unlike the oscillations of the "spin flavor," in the case of neutrino oscillations, we have not two, but three mass states with definite values of rest energy $m_k c^2$, where k = 1, 2, 3. The important consequence of neutrino oscillations is that they represent a significant deviation from the Standard Model of particle physics [10]. In the Standard Model, neutrinos have zero rest mass (like a photon) and all propagate with the speed of light.

Mathematically, the neutrino flavor states are expressed in terms of the mass states using the 3 × 3 lepton mixing matrix $U_{\alpha k}$ [11]:

$$|\nu_\alpha\rangle = \sum U^*_{\alpha k}|k\rangle. \quad (7)$$

In this and the following expressions, the sum is taken over the mass index k = 1, 2, 3. If a neutrino is created in the flavor state $|\alpha\rangle$, the probability of observing it in a flavor state $\left|\alpha'\right\rangle$ is given by the expression:

$$P_{\alpha\alpha'} = \left|\sum U^*_{\alpha k} U_{\alpha' k} \exp\left(-\frac{i m_k^2 c^3 d}{\hbar E}\right)\right|^2. \quad (8)$$

Here, d is the distance from the neutrino source, and E is the total relativistic neutrino energy. Note that Equation (8) was derived assuming the ultra-relativistic limit: $m_k c^2 << E$.

Neutrino oscillation experiments reliably indicate three mass states. Analysis of the available cosmological data provides the following bounds on the sum of the masses of these states: 60 meV < $(m_1 + m_2 + m_3)c^2$ < 110 meV [12]. These bounds are, however, cosmological model-dependent. The measurement of the absolute value of the neutrino and antineutrino masses is a notoriously complicated problem. The most advanced Karlsruhe Tritium Neutrino (KATRIN) experiment measures the energy distribution of electrons emitted in the process of tritium beta decay. The latest report gives an upper limit for the electron antineutrino rest energy of 450 meV [13]. Note that there are two possible arrangements for the values of the mass states: (1) $m_1 < m_2 < m_3$ (normal ordering), and (2) $m_3 < m_1 < m_2$ (inverted ordering). Current experiments cannot determine which ordering is correct. For the normal ordering, the rest energy squared differences are found to be $(m_2^2 - m_1^2)c^4 = 7.4 \times 10^{-5}$ $(eV)^2$ and $(m_3^2 - m_1^2)c^4 = 2.5 \times 10^{-3}$ $(eV)^2$ [14]. For the inverted ordering, the first difference remains the same, while the second one changes to $(m_2^2 - m_3^2)c^4 = 2.5 \times 10^{-3}$ $(eV)^2$. In any case, these data imply that the mass states have a maximum rest energy greater than 50 meV.

A non-zero neutrino mass poses serious challenges for the theory of neutrinos. First of all, for massless particles, the helicity, i.e., the spin component relative to the particle's momentum, is equivalent to chirality, which is a fundamental property associated with the asymmetry between a quantum field and its mirror image [15]. For a massive particle, which moves with a speed less than the speed of light, the helicity depends on the reference frame, while the chirality does not depend on the reference frame. The weak interaction generates Dirac neutrinos and antineutrinos of definite chirality: left-handed Dirac neutrinos and right-handed Dirac antineutrinos. In principle, for a massive neutrino, the weak interaction may produce neutrinos with left-handed chirality but right-handed

helicity. Nevertheless, for ultra-relativistic neutrinos (the rest energy is much smaller than the total relativistic energy), the probability of this event is negligible. When a neutrino with non-zero mass moves in a free space, its helicity does not change. However, the chirality of a freely moving neutrino with non-zero mass is not conserved, and so may change. Thus, a neutrino with left-handed chirality and left-handed helicity, while moving through free space, may transform into a neutrino with right-handed chirality and left-handed helicity. Again, the probability of this transformation is negligible for ultra-relativistic neutrinos. In conclusion, for ultra-relativistic neutrinos and antineutrinos, one can safely ignore the fundamental difference between chirality and helicity.

Various extensions of the Standard Model of particle physics predict the existence of additional flavors of right-handed "sterile neutrinos" and left-handed "sterile antineutrinos", which do not participate in the weak interaction [16–18]. While difficult to estimate, the rest masses of sterile neutrinos are expected to be much greater than the masses of the mass states (m_1, m_2, and m_3) whose superpositions form the "active neutrinos", i.e., the electron, muon, and tau neutrinos. If neutrinos are Majorana fermions, then in nuclear beta decays, the active Majorana neutrinos with left-handed chirality could be generated with a small admixture of sterile neutrinos with right-handed chirality.

The search for sterile neutrinos is an important area of research. Experiments with the Los Alamos Liquid Scintillator Detector (LSND) and the Mini Booster Neutrino Experiment (MiniBooNE) indicated the existence of sterile neutrinos with rest energy about 1 eV, but these results were not confirmed by other experiments [19]. The well-known cosmic X-ray line radiation, with energy of approximately 3.5 keV, was found to be consistent with dark matter sterile neutrinos of 7 keV rest energy [20]. The constraints on sterile neutrinos with rest energy in the MeV–GeV range are discussed, for example, in ref. [21].

In our paper, we consider the search for sterile neutrinos with rest energy in the approximate range 100–400 keV, using electron capture beta decay. In electron capture beta decay, an atomic nucleus of atomic number Z and electric charge Ze absorbs an electron from one of the atomic S-orbitals, transforming into a nucleus of atomic number (Z−1) and radiating an electron neutrino:

$$Z + e^- \rightarrow (Z - 1) + \nu_e. \quad (9)$$

This means that a proton in the nucleus absorbs an electron, transforms into a neutron, and radiates an electron neutrino. On a more fundamental level, due to the weak interaction, an up quark in the proton absorbs an electron and transforms into a down quark while radiating an electron neutrino. It has been suggested that the electron neutrino radiated in this process may have a small admixture of a sterile neutrino [22]. Indeed, assume that the mass of the sterile neutrino is smaller than the nuclear decay energy released in the capture process (i.e., the "Q value"). Also, assume that the change in the recoil energy, associated with the radiation of a sterile rather than an active electron neutrino, is much greater than the measurement uncertainty of the recoil energy. Under these conditions, we may detect the emission of a massive sterile neutrino. Even if the amplitude of the sterile neutrino in the original wave function is very small, there will be a finite probability that the atom radiates a heavy sterile neutrino. In this case, the recoil energy of the daughter atom will be smaller than that in the case of radiation of an electron neutrino. In ref. [22], the authors reported a search for sterile neutrinos of rest energy from 370 keV to 640 keV using the electron capture beta decay $^{37}Ar \rightarrow {}^{37}Cl$. In this decay, the atomic number Z changes from 18 to 17. The recoil energies of the daughter ^{37}Cl atoms were measured in the region of 3.6 eV to 7.6 eV. Electron capture beta decays $^{7}Be \rightarrow {}^{7}Li$, and $^{131}Cs \rightarrow {}^{131}Xe$ were identified as the best candidates for the search for sterile neutrinos [23]. In particular, ^{7}Be is

the lightest atom that decays by electron capture. The daughter ^{7}Li atom has a relatively large recoil energy, which is very important in the search for a sterile neutrino.

Improvements in detector technology and the ability to implant radioisotopes directly into the detectors have triggered a resurgence of nuclear recoil experiments (see for example, [24]). In ref. [25], the authors used the Isotope Separator and Accelerator (ISAC) in Vancouver, Canada, to implant ^{7}Be atoms into superconducting tunnel junction sensors (STJ). In an STJ, two superconductors are separated by a barrier, like in a Josephson junction. When a daughter ^{7}Li atom deposits its recoil energy in the detector, electrons are excited above the small (about 1 meV) superconducting energy gap. The increase in current due to the excited electrons is proportional to the recoil energy. This technique allowed the authors of [25] to carry out a search for sterile neutrinos with rest energy in the region of 100 keV to 850 keV.

In this paper, we report a comprehensive analysis of the two channels of ^{7}Be electron capture beta decay. In the first (one-step) channel, the ^{7}Be nucleus captures an electron and decays to the nuclear ground state of the daughter ^{7}Li atom, radiating a neutrino. In the second (two-step) channel, the ^{7}Be nucleus captures an electron and decays to the excited state of the ^{7}Li nucleus, radiating a neutrino, and then the ^{7}Li nucleus transfers to its ground state, radiating a γ-ray photon. For both channels, we find the recoil energy assuming radiation of a massive neutrino. We derive analytical expressions for the recoil energy and discuss opportunities for exploiting the two-step channel in searches for sterile neutrinos in electron capture beta decays.

2. Materials and Methods

We consider the electron capture beta decay $^7\text{Be} \rightarrow {}^7\text{Li}$, illustrated in Figure 1.

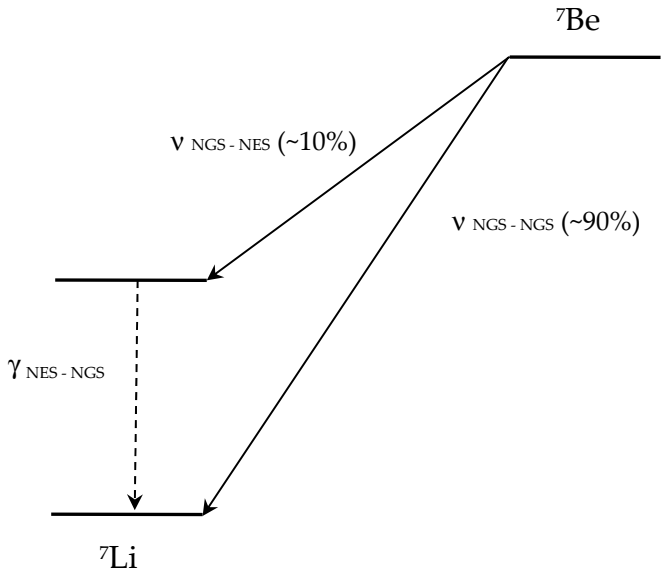

Figure 1. Schematic energy level diagram showing the basic features of the ^{7}Be electron capture decay. Neutrinos are emitted with energies characteristic of a nuclear parent ground state to nuclear daughter ground state decay ($_{\text{NGS-NGS}}$) and of a nuclear parent ground state to nuclear daughter excited state decay ($_{\text{NGS-NES}}$). The latter is promptly followed by a high energy γ-ray emission ($_{\text{NES-NGS}}$).

About 90% of ^{7}Be nuclei decay to the nuclear ground state of ^{7}Li ($_{\text{NGS-NGS}}$), while about 10% decay into the nuclear excited state ($_{\text{NGS-NES}}$) and then transition to the nuclear ground state, radiating a γ-ray photon ($_{\text{NES-NGS}}$). We consider the recoil energies of the daughter ^{7}Li atoms for these two channels.

First, we consider the one-step decay channel: an electron capture in a parent ^{7}Be atom with a direct decay to the nuclear ground state of the daughter ^{7}Li atom. The conceptually simplest situation occurs for an L-capture, i.e., the capture of an outer 2s-electron. After the capture of an outer L electron, the electronic system of the daughter atom will likely be in its ground state $1s^2 2s^1$. After a K-capture, i.e., the capture of a 1s-electron, the nucleus transfers to its ground state, but the electronic system will likely be in the excited state $1s^1 2s^2$. We focus on these two final electronic states and omit consideration of complicating background situations where the daughter is left in some higher excited state (shake-ups) or is ionized (shake-offs). In a shake-up, the sudden change in the nuclear charge in the process of nuclear decay causes the ^{7}Li atom to transition to a higher excited state. In a shake-off, the sudden change in the nuclear charge causes ionization of the ^{7}Li atom. These effects do not cause a noticeable change in the recoil energy of a daughter atom, as shown in recent experiments [25,26]. The K and L recoil spectra were resolved and the shake-up and shake-off contributions identified, allowing use of the results of our computations for both K- and L-captures.

To begin, we assume that a radioactive ^{7}Be atom at rest absorbs an s-electron, radiating a neutrino. Let the rest mass of the daughter ^{7}Li atom with the nucleus in the ground state be M_{Li}, the rest mass of the emitted neutrino be M_ν, the energy difference between the initial rest energy of the parent ^{7}Be atom and the final rest energy of the daughter atom be Q, the relativistic energy of the emitted neutrino be E_ν, and the relativistic energy of the recoiling daughter atom be E_{Li}. From energy conservation, we obtain

$$M_{Li}c^2 + Q = E_\nu + E_{Li}. \tag{10}$$

Let the magnitude of the neutrino momentum be p_ν and the magnitude of the recoil momentum of the ^{7}Li atom be p_{Li}. Then the relativistic energies of a neutrino of rest mass M_ν, and the daughter atom of rest mass M_{Li}, are given by the expressions

$$E_\nu = \sqrt{M_\nu^2 c^4 + p_\nu^2 c^2}, \qquad E_{Li} = \sqrt{M_{Li}^2 c^4 + p_{Li}^2 c^2}. \tag{11}$$

From momentum conservation, the magnitude of the neutrino momentum equals the magnitude of the atomic recoil momentum: $p_{Li} = p_\nu$.

Secondly, we consider the two-step decay channel: the ^{7}Be nucleus captures an s-electron, radiates a neutrino, and decays to the nuclear excited state of ^{7}Li. Then, the ^{7}Li nucleus promptly transfers to its ground state, radiating a γ-ray photon. We assume that the lifetime of the nuclear excited state is much shorter than the measurement time of the recoil energy of the ^{7}Li atom. After the neutrino radiation, the nucleus of the daughter ^{7}Li atom will be in its excited state. The rest mass of the ^{7}Li atom after neutrino radiation, we denote as M_{Li^*}, the momentum p_{Li^*}, and the relativistic energy E_{Li^*}. The relation between the energy, rest mass, and momentum of the ^{7}Li atom in the excited nuclear state is described by the relativistic expression

$$E_{Li^*} = \sqrt{M_{Li^*}^2 c^4 + c^2 p_{Li^*}^2}. \tag{12}$$

From energy conservation, we have,

$$M_{Li}c^2 + Q = E_\nu + E_{Li^*}, \tag{13}$$

and, from momentum conservation, $p_{Li^*} = p_\nu$.

Following radiation of the γ-ray photon, the ^{7}Li nucleus transfers to its ground state. For the ^{7}Li atom, with its nucleus in the ground state, we use the same notations E_{Li} and

p_{Li} as we did for the one-step channel. If we denote the momentum of the radiated photon as p_γ, and its energy as $E_\gamma = cp_\gamma$, then from energy conservation, we have

$$E_{Li^*} = E_{Li} + E_\gamma. \tag{14}$$

From momentum conservation, we obtain the vector equation,

$$\vec{p_{Li^*}} = \vec{p_{Li}} + \vec{p_\gamma}. \tag{15}$$

Taking into consideration that $p_{Li^*} = p_\nu$, we obtain from Equation (15):

$$p_{Li} = \sqrt{(p_\nu + p_\gamma \cos\theta)^2 + p_\gamma^2 \sin^2\theta}. \tag{16}$$

Here θ is the angle between the directions of motion of the neutrino and the photon, such that $\theta = 0$ corresponds to the case where the neutrino and the photon are emitted in the same direction. In the next section, based only on the conservation of energy and momentum, we obtain exact analytical expressions for the recoil energy of the daughter ^{7}Li atom in both channels.

3. Results

In this section, we perform analytical computations and numerical estimates of the recoil kinetic energy of the daughter ^{7}Li atom.

3.1. Recoil Energy in the One-Step Decay Channel

3.1.1. Radiation of a Massless Neutrino

First, we obtain the analytical formula for the recoil energy of the ^{7}Li atom assuming that a massive neutrino does not exist. In this case, we can ignore the neutrino mass and take $M_\nu = 0$. We begin with the equation,

$$M_{Li}c^2 + Q = p_\nu c + E_{Li}. \tag{17}$$

By rearranging this equation and squaring, we obtain,

$$\left(M_{Li}c^2 + Q - E_{Li}\right)^2 = p_\nu^2 c^2. \tag{18}$$

Taking $p_\nu^2 c^2$ from the formula, $E_{Li} = \sqrt{M_{Li}^2 c^4 + p_\nu^2 c^2}$, and expanding we find

$$\left(M_{Li}c^2 + Q\right)^2 - 2E_{Li}\left(M_{Li}c^2 + Q\right) + E_{Li}^2 = E_{Li}^2 - M_{Li}^2 c^4. \tag{19}$$

From this equation we have,

$$\left(M_{Li}c^2 + Q\right)^2 + M_{Li}^2 c^4 = 2E_{Li}\left(M_{Li}c^2 + Q\right). \tag{20}$$

Finally, we obtain the expression for the relativistic energy of the ^{7}Li atom:

$$E_{Li} = \frac{\left(M_{Li}c^2 + Q\right)^2 + M_{Li}^2 c^4}{2(M_{Li}c^2 + Q)}. \tag{21}$$

The kinetic recoil energy of the ^{7}Li atom K_{Li} can be found by subtracting its rest energy:

$$K_{Li} = E_{Li} - M_{Li}c^2. \tag{22}$$

Therefore,

$$K_{Li} = \frac{\left(M_{Li}c^2 + Q\right)^2 + M_{Li}^2c^4}{2(M_{Li}c^2 + Q)} - M_{Li}c^2. \tag{23}$$

It can be rewritten as

$$K_{Li} = \frac{Q^2}{2(M_{Li}c^2 + Q)}, \tag{24}$$

giving a compact expression for the recoil kinetic energy with a massless neutrino in the one-step decay channel.

3.1.2. Radiation of a Massive Neutrino

The one-step channel with emission of a massive neutrino is governed by the three equations:

$$E_\nu = \sqrt{M_\nu^2c^4 + p_\nu^2c^2},\ E_{Li} = \sqrt{M_{Li}^2c^4 + p_\nu^2c^2},\ M_{Li}c^2 + Q = E_\nu + E_{Li}. \tag{25}$$

From the first two equations in (25) we notice that

$$E_{Li}^2 - M_{Li}^2c^4 + M_\nu^2c^4 = E_\nu^2. \tag{26}$$

From the third equation in (25) we obtain,

$$\left(M_{Li}c^2 + Q - E_{Li}\right)^2 = E_\nu^2. \tag{27}$$

Expanding this expression and using Equation (26) we find,

$$\left(M_{Li}c^2 + Q\right)^2 - 2E_{Li}\left(M_{Li}c^2 + Q\right) + E_{Li}^2 = E_{Li}^2 - M_{Li}^2c^4 + M_\nu^2c^4. \tag{28}$$

The last equation can be simplified to give:

$$\left(M_{Li}c^2 + Q\right)^2 + M_{Li}^2c^4 - M_\nu^2c^4 = 2E_{Li}\left(M_{Li}c^2 + Q\right). \tag{29}$$

From here we obtain the expression for the relativistic energy of the ^{7}Li atom:

$$E_{Li} = \frac{\left(M_{Li}c^2 + Q\right)^2 + M_{Li}^2c^4 - M_\nu^2c^4}{2(M_{Li}c^2 + Q)}. \tag{30}$$

The recoil kinetic energy of the ^{7}Li atom is given by,

$$K_{Li} = E_{Li} - M_{Li}c^2 = \frac{Q^2 - M_\nu^2c^4}{2(M_{Li}c^2 + Q)}. \tag{31}$$

This expression is the same as that already available in the literature [25]. Note that the recoil kinetic energy approaches zero when the neutrino rest energy $M_\nu c^2$ approaches Q. When $M_\nu c^2 = Q$ the entire energy of nuclear decay transforms into the rest energy of the neutrino with no residual kinetic energy. The rest energy of a radiated massive neutrino certainly cannot be greater than Q.

3.2. Recoil Energy in the Two-Step Decay Channel

In this subsection we obtain analytical expressions describing the recoil energy in the two-step channel. First, we consider the decay with radiation of a neutrino with zero rest mass, and secondly with radiation of a massive neutrino.

3.2.1. Radiation of a Massless Neutrino and a γ-Ray Photon

We now find the final recoil kinetic energy of the daughter atom after radiation of a massless neutrino and a γ-ray photon. After radiation of a massless neutrino, we have from energy conservation:

$$M_{Li}c^2 + Q = p_\nu c + E_{Li^*}. \tag{32}$$

From this equation we obtain,

$$\left(M_{Li}c^2 + Q - E_{Li^*}\right)^2 = p_\nu^2 c^2. \tag{33}$$

Using Equation (12) for the relativistic energy E_{Li^*}, we express $p_\nu^2 c^2$ in terms of E_{Li^*} to obtain

$$\left(M_{Li}c^2 + Q\right)^2 - 2E_{Li^*}\left(M_{Li}c^2 + Q\right) + E_{Li^*}^2 = E_{Li^*}^2 - M_{Li^*}^2 c^4. \tag{34}$$

We can rewrite this equation in the following form:

$$\left(M_{Li}c^2 + Q\right)^2 + M_{Li^*}^2 c^4 = 2E_{Li^*}\left(M_{Li}c^2 + Q\right). \tag{35}$$

From the last equation we obtain an expression for the relativistic energy E_{Li^*}:

$$E_{Li^*} = \frac{\left(M_{Li}c^2 + Q\right)^2 + M_{Li^*}^2 c^4}{2(M_{Li}c^2 + Q)}. \tag{36}$$

A similar derivation provides the expression for $p_\nu c$. Beginning from Equation (32), we obtain

$$\left(M_{Li}c^2 + Q - p_\nu c\right)^2 = E_{Li^*}^2. \tag{37}$$

Substituting expression (12) for the relativistic energy E_{Li^*} we obtain,

$$\left(M_{Li}c^2 + Q\right)^2 - 2p_\nu c\left(M_{Li}c^2 + Q\right) + p_\nu^2 c^2 = p_\nu^2 c^2 + M_{Li^*}^2 c^4. \tag{38}$$

We can rewrite the last equation in the form,

$$\left(M_{Li}c^2 + Q\right)^2 - M_{Li^*}^2 c^4 = 2p_\nu c\left(M_{Li}c^2 + Q\right). \tag{39}$$

From here we obtain an expression for $p_\nu c$:

$$p_\nu c = \frac{\left(M_{Li}c^2 + Q\right)^2 - M_{Li^*}^2 c^4}{2(M_{Li}c^2 + Q)}. \tag{40}$$

Now, we consider the second step of the decay, ultimately arriving at an expression for K_{Li}. From energy conservation,

$$E_{Li^*} = E_{Li} + p_\gamma c. \tag{41}$$

We rewrite this equation in the form

$$(E_{Li^*} - p_\gamma c)^2 = E_{Li}^2. \tag{42}$$

Substituting the expression for the relativistic energy E_{Li} we find

$$E_{Li^*}^2 - 2p_\gamma c E_{Li^*} + p_\gamma^2 c^2 = M_{Li}^2 c^4 + p_{Li}^2 c^2. \tag{43}$$

Substituting Equation (16) for p_{Li} we obtain

$$E_{Li^*}^2 - 2p_\gamma c E_{Li^*} + p_\gamma^2 c^2 = M_{Li}^2 c^4 + (p_\nu + p_\gamma cos\theta)^2 c^2 + p_\gamma^2 c^2 sin^2\theta. \quad (44)$$

We simplify this equation to get

$$2p_\gamma c E_{Li^*} + 2p_\nu p_\gamma c^2 \cos\theta = E_{Li^*}^2 - M_{Li}^2 c^4 - p_\nu^2 c^2. \quad (45)$$

Substituting Equation (12) for the relativistic energy E_{Li^*}, we obtain

$$2p_\gamma c * (E_{Li^*} + p_\nu c \cos\theta) = M_{Li^*}^2 c^4 - M_{Li}^2 c^4. \quad (46)$$

From here we find an expression for $p_\gamma c$:

$$p_\gamma c = \frac{M_{Li^*}^2 c^4 - M_{Li}^2 c^4}{2(E_{Li^*} + p_\nu c \cos\theta)}. \quad (47)$$

where E_{Li^*} is given by Equation (36) and $p_\nu c$ by Equation (40). Note that this equation can be used to determine the angle θ between the directions of propagation of the neutrino and the γ-ray photon by measuring the photon energy $p_\gamma c$.

Now that the expression for $p_\gamma c$ is derived, the relativistic energy E_{Li} can be easily found using Equation (41):

$$E_{Li} = E_{Li^*} - p_\gamma c. \quad (48)$$

The recoil kinetic energy K_{Li} is then given by:

$$K_{Li} = E_{Li^*} - p_\gamma c - M_{Li} c^2, \quad (49)$$

where the first term on the right side of the formula is given by Equation (36) and the second term by Equation (47).

We now consider the special case of the maximum recoil kinetic energy when a photon is radiated in the same direction as the neutrino: $\theta = 0$. We use our expressions (36), (47) and (49) with $\theta = 0$. Substituting expressions (47) and (36) for $p_\gamma c$ and E_{Li^*} into Equation (49), we obtain,

$$K_{Li} = \frac{(M_{Li}c^2 + Q)^2 + M_{Li^*}^2 c^4}{2(M_{Li}c^2 + Q)} - \frac{M_{Li^*}^2 c^4 - M_{Li}^2 c^4}{2(E_{Li^*} + p_\nu c \cos 0)} - M_{Li}c^2. \quad (50)$$

From Equation (32), we can rewrite the denominator in the second term on the right side of this equation:

$$K_{Li} = \frac{(M_{Li}c^2 + Q)^2 + M_{Li^*}^2 c^4}{2(M_{Li}c^2 + Q)} - \frac{M_{Li^*}^2 c^4 - M_{Li}^2 c^4}{2(M_{Li}c^2 + Q)} - M_{Li}c^2. \quad (51)$$

The last equation can then be written as

$$K_{Li} = \frac{(M_{Li}c^2 + Q)^2 + M_{Li}^2 c^4}{2(M_{Li}c^2 + Q)} - M_{Li}c^2, \quad (52)$$

which simplifies to expression (24). Thus, we obtained the same formula as for the recoil kinetic energy in the one-step decay channel. This means that, for a neutrino with zero rest mass, the maximum recoil energy in the two-step channel exactly equals the recoil energy in the one-step channel.

3.2.2. Radiation of a Massive Neutrino and a γ-Ray Photon

Now we consider the situation when a radioactive ^{7}Be nucleus decays to a ^{7}Li nucleus in its excited state radiating a massive neutrino, then the ^{7}Li nucleus transfers to its ground state, radiating a γ-ray photon. We analyze the first step, then the second step, and then derive an expression for the final recoil kinetic energy. Beginning from expressions for the relativistic energies (11) and (12) we obtain,

$$E_{Li^*}^2 - M_{Li^*}^2 c^4 + M_\nu^2 c^4 = E_\nu^2. \tag{53}$$

Next, from the conservation of energy (Equation (13)) we have,

$$\left(M_{Li}c^2 + Q - E_{Li^*}\right)^2 = E_\nu^2. \tag{54}$$

From these two equations,

$$\left(M_{Li}c^2 + Q\right)^2 - 2E_{Li^*}\left(M_{Li}c^2 + Q\right) + E_{Li^*}^2 = E_{Li^*}^2 - M_{Li^*}^2 c^4 + M_\nu^2 c^4. \tag{55}$$

We can write the last equation in the form,

$$\left(M_{Li}c^2 + Q\right)^2 + M_{Li^*}^2 c^4 - M_\nu^2 c^4 = 2E_{Li^*}\left(M_{Li}c^2 + Q\right). \tag{56}$$

From here, we find the equation for E_{Li^*}:

$$E_{Li^*} = \frac{\left(M_{Li}c^2 + Q\right)^2 + M_{Li^*}^2 c^4 - M_\nu^2 c^4}{2(M_{Li}c^2 + Q)}. \tag{57}$$

A similar derivation provides an expression for E_ν. From Equation (13), we obtain

$$\left(M_{Li}c^2 + Q - E_\nu\right)^2 = E_{Li^*}^2 \tag{58}$$

Substituting expression (53) for $E_{Li^*}^2$ we have

$$\left(M_{Li}c^2 + Q\right)^2 - 2E_\nu\left(M_{Li}c^2 + Q\right) + E_\nu^2 = E_\nu^2 - M_\nu^2 c^4 + M_{Li^*}^2 c^4. \tag{59}$$

The last equation we can rewrite in the form

$$\left(M_{Li}c^2 + Q\right)^2 - M_{Li^*}^2 c^4 + M_\nu^2 c^4 = 2E_\nu\left(M_{Li}c^2 + Q\right). \tag{60}$$

From here, we obtain the expression for E_ν:

$$E_\nu = \frac{\left(M_{Li}c^2 + Q\right)^2 - M_{Li^*}^2 c^4 + M_\nu^2 c^4}{2(M_{Li}c^2 + Q)}. \tag{61}$$

Now, we consider the second step of the decay, ultimately arriving at an expression for K_{Li}. Again, we begin with conservation of energy,

$$E_{Li^*} = E_{Li} + p_\gamma c. \tag{62}$$

By rearranging the equation and squaring,

$$(E_{Li^*} - p_\gamma c)^2 = E_{Li}^2. \tag{63}$$

Substituting Equation (11) for E_{Li} we obtain,

$$E_{Li^*}^2 - 2p_\gamma c E_{Li^*} + p_\gamma^2 c^2 = M_{Li}^2 c^4 + p_{Li}^2 c^2. \quad (64)$$

Next, substituting Equation (16) for p_{Li}, we have

$$E_{Li^*}^2 - 2p_\gamma c E_{Li^*} + p_\gamma^2 c^2 = M_{Li}^2 c^4 + (p_\nu + p_\gamma cos\theta)^2 c^2 + p_\gamma^2 c^2 sin^2\theta. \quad (65)$$

Expanding, we obtain,

$$E_{Li^*}^2 - 2p_\gamma c E_{Li^*} + p_\gamma^2 c^2 = M_{Li}^2 c^4 + p_\nu^2 c^2 + 2p_\nu p_\gamma c^2 \cos\theta + p_\gamma^2 c^2 cos^2\theta + p_\gamma^2 c^2 \sin^2\theta. \quad (66)$$

From the last equation we obtain

$$2p_\gamma c E_{Li^*} + 2p_\nu p_\gamma c^2 \cos\theta = E_{Li^*}^2 - M_{Li}^2 c^4 - p_\nu^2 c^2. \quad (67)$$

Substituting Equation (12) for $E_{Li^*}^2$, where $p_{Li^*} = p_\nu$, we find the equation

$$2p_\gamma c * (E_{Li^*} + p_\nu c \cos\theta) = M_{Li^*}^2 c^4 - M_{Li}^2 c^4. \quad (68)$$

where $p_\nu c = \sqrt{E_\nu^2 - M_\nu^2 c^4}$.

This equation yields an expression for $p_\gamma c$:

$$p_\gamma c = \frac{M_{Li^*}^2 c^4 - M_{Li}^2 c^4}{2(E_{Li^*} + \sqrt{E_\nu^2 - M_\nu^2 c^4} \cdot \cos\theta)}. \quad (69)$$

Now that an expression for $p_\gamma c$ has been derived, the relativistic energy E_{Li} can be easily computed:

$$E_{Li} = E_{Li^*} - p_\gamma c. \quad (70)$$

Finally, the recoil kinetic energy K_{Li} for the two-step decay is given by Equation (49), where E_{Li^*} can be found from Equation (57) and $p_\gamma c$ from Equation (69).

3.3. Numerical Estimates

In this subsection, we estimate the recoil kinetic energy of the ^{7}Li atom assuming that the rest energy of the postulated sterile neutrino is $M_\nu c^2 = 300$ keV. We use the following values of parameters available in the literature [27]: the rest energy difference between the original state of the ^{7}Be atom and the final state of the ^{7}Li atom $Q = 861.89 \pm 0.07$ keV, the rest energy difference between the ^{7}Li atom with the excited nuclear state and the final state of the ^{7}Li atom

$$(M_{Li^*} - M_{Li})c^2 = 477.612 \pm 3 \times 10^{-3} \text{ keV}, \quad (71)$$

and the rest energy of the final state of the ^{7}Li atom $M_{Li}c^2 = 6.53537 \pm 5 \times 10^{-9}$ GeV.

Using these values, for the one-step channel, we obtained the following estimates: after radiation of a massless neutrino, $K_{Li} \approx 56.8$ eV, and after radiation of a 300 keV massive sterile neutrino, $K_{Li} \approx 49.9$ eV.

In Figure 2, we present the Li recoil kinetic energy K_{Li} (in eV) as a function of the angle θ (in radians) for both channels. The blue dotted curve shows the recoil energy after emission of a 300 keV neutrino, and the black dotted curve corresponds to emission of a massless neutrino. One can see that the recoil energy monotonically decreases as θ increases. The horizontal solid lines show the values of the recoil energy for the one-step

decay: blue line for a 300 keV neutrino, and black line for a massless neutrino. The error bars correspond to the experimental uncertainty of 2.9 eV reported in ref. [28].

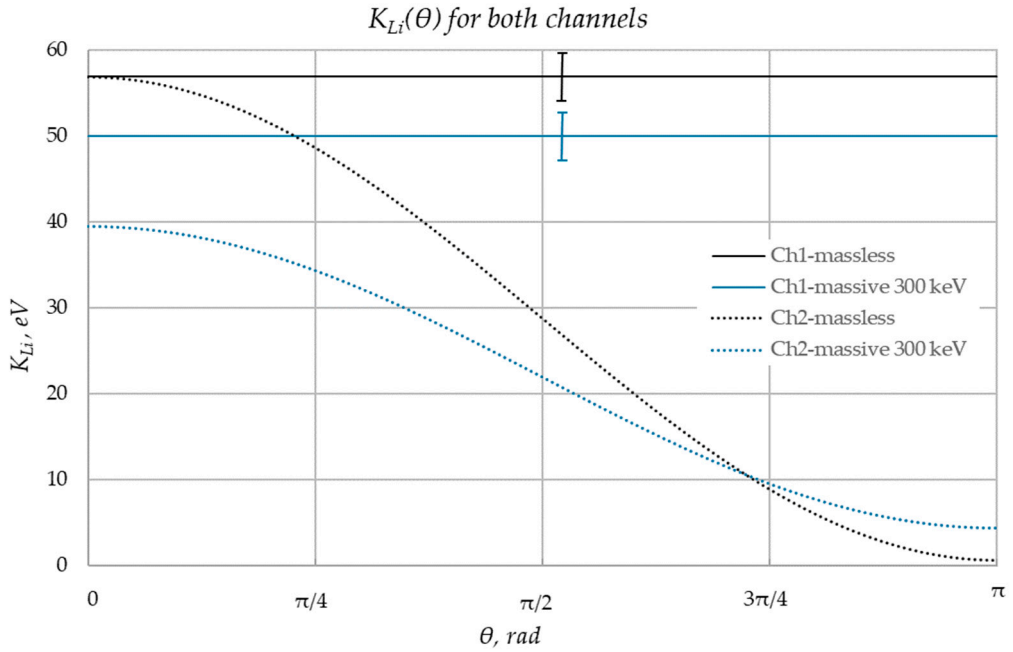

Figure 2. Graphs of the Li recoil kinetic energy $K_{Li}(\theta)$. The one-step channel with emission of a 300 keV sterile neutrino-blue solid line (Ch1-massive 300 keV); the one-step channel with emission of a massless neutrino-black solid line (Ch1-massless); the two-step channel with emission of a 300 keV sterile neutrino and a photon–dotted blue line (Ch2-massive 300 keV); the two-step channel with emission of a massless neutrino and a photon-dotted black line (Ch2-massless).

As we showed above, in the case of radiation of a massless neutrino, the maximum recoil energy of the ^{7}Li atom for the two-step channel (which corresponds to $\theta = 0$) is exactly the same as the recoil energy for the one-step channel, i.e., 56.8 eV. The situation changes when a 300 keV sterile neutrino is radiated. In this case, the recoil energy in the two-step channel is 39.4 eV, i.e., significantly smaller than that in the one-step channel. The difference between the maximum recoil energy in the two-step channel and the recoil energy in the one-step channel increases from zero to 10.5 eV. The measurement error for the difference of two recoil energies is expected to have a smaller value: 2×2.9 eV = 5.8 eV. Thus, this difference could potentially be exploited for the detection of sterile neutrinos.

Next, we consider the difference between the maximum and minimum recoil energies in the two-step channel. The minimum recoil energy corresponds to $\theta = \pi$, when the photon and neutrino are emitted in opposite directions. For a massless neutrino, the minimum recoil energy is, approximately, 0.667 eV, while for a 300 keV neutrino, this value is 4.31 eV. The difference between the maximum and minimum recoil energies for a massless neutrino is, approximately 56.1 eV, while for a 300 keV neutrino, it has a much smaller value of 35.1 eV, both with the expected measurement error of 5.8 eV. This change could also potentially be exploited for the detection of a sterile neutrino.

4. Discussion

In this paper, we studied the recoil energy of the ^{7}Li atom after the electron capture beta decay of a radioactive ^{7}Be atom. We were interested in the opportunity to use the recoil energy in the search for a massive sterile neutrino, which could be mixed with the electron neutrino radiated in the nuclear decay process. We considered two channels of the decay. In the first one-step channel, the ^{7}Be nucleus directly decays to the ground state of the ^{7}Li

nucleus, radiating a neutrino. In the second two-step channel, the ^{7}Be nucleus decays to the excited state of the ^{7}Li nucleus, radiating a neutrino; then, the ^{7}Li nucleus transfers to its ground state, radiating a γ-ray photon. We assume that in both channels, the recoil energy of the ^{7}Li atom is measured after the ^{7}Li nucleus comes to its ground state. In the case of an L-capture (capture of a 2s-electron), after the nuclear decay, the electron shell of the daughter ^{7}Li atom likely comes to its ground state $1s^2 2s^1$. For the case of the K-capture (capture of a 1s-electron), the electron shell likely comes to the excited state $1s^1 2s^2$, which is usually followed by emission of an Auger electron [25]. For the one-step channel, our result confirms the formula published previously in [25]. For the two-step channel, to the best of our knowledge, the exact analytical expressions for the recoil kinetic energy have not been published before.

Based on the results of our computations, we wish to discuss the opportunities to exploit the two-step electron capture beta decay of a ^{7}Be atom in order to detect a sterile neutrino by measuring the recoil energy of the daughter ^{7}Li atom. We assume that the rest energy of the sterile neutrino is smaller than the decay energy released in the first step of the two-step decay (approximately, 384 keV). In this case, we expect a small but finite probability that the electron neutrino generated in the first step of the nuclear decay collapses into a sterile neutrino. We wish to attract the attention of experimentalists to two possibilities for the detection of a sterile neutrino.

1. The difference between the recoil energies in the one-step decay and the maximum recoil energy in the two-step decay is exactly zero for emission of a massless neutrino and has a finite value for emission of a massive neutrino. We showed that this value may be greater than the uncertainty of the recoil energy.
2. The difference between the maximum and the minimum recoil energies in the two-step decay changes significantly if a massive neutrino is emitted. We showed that this change may also be greater than the measurement uncertainty.

In conclusion, we should mention that our results can be applied to any electron capture isotope with a similar two-channel decay mode.

Author Contributions: All the authors equally contributed to the article. All authors have read and agreed to the published version of the manuscript.

Funding: This research received no external funding.

Data Availability Statement: The original contributions presented in the study are included in the article; further inquiries can be directed to the corresponding author.

Acknowledgments: We are thankful to Valery Sheverev for his support and useful discussions.

Conflicts of Interest: The authors declare no conflicts of interest.

Abbreviations

The following abbreviations are used in this manuscript:

LHC	Large Hadron Collider
FASER	ForwArd Search ExpeRiment
LSND	Los Alamos Liquid Scintillator Detector
MiniBooNE	Mini Booster Neutrino Experiment
ISAC	Isotope Separator and Accelerator
STJ	Superconducting tunnel junction sensors
NGS	Nuclear ground state
NES	Nuclear excited state

References

1. Lesgourgues, J.; Mangano, G.; Miele, G.; Pastor, S. *Neutrino Cosmology*; Cambridge University Press: Cambridge, UK, 2013.
2. Follin, B.; Knox, L.; Millea, M.; Pan, Z. First Detection of the Acoustic Oscillation Phase Shift Expected from the Cosmic Neutrino Background. *Phys. Rev. Lett.* **2015**, *115*, 091301. [CrossRef]
3. Kaye, G.W.C.; Laby, T.H. Nuclear Fission and Fusion, and Neutron Interactions. In *Tables of Physical and Chemical Constants and Some Mathematical Functions*, 16th ed.; Longman Scientific & Technical: Essex, UK, 1995.
4. Agostini, M.; Appel, S.; Bellini, G.; Benziger, J.; Bick, D.; Bonfini, G.; Bravo, D.; Caccianiga, B.; Calaprice, F.; Caminata, A.; et al. Spectroscopy of Geoneutrinos from 2056 Days of Borexino Data. *Phys. Rev. D* **2015**, *92*, 031101. [CrossRef]
5. Abbasi, R.; Abdou, Y.; Abu-Zayyad, T.; Adams, J.; Aguilar, J.A.; Ahlers, M.; Andeen, K.; Auffenberg, J.; Bai, X.; Baker, M.; et al. The Energy Spectrum of Atmospheric Neutrinos between 2 and 200 TeV with the AMANDA-II Detector. *Astropart. Phys.* **2010**, *34*, 48–58. [CrossRef]
6. Kopp, S. Accelerator Neutrino Beams. *Phys. Rep.* **2007**, *439*, 101–159. [CrossRef]
7. Abreu, H.; Afik, Y.; Antel, C.; Arakawa, J.; Ariga, A.; Ariga, T.; Bernlochner, F.; Boeckh, T.; Boyd, J.; Brenner, L.; et al. First Neutrino Interaction Candidates at the LHC. *Phys. Rev. D* **2021**, *104*, L091101. [CrossRef]
8. Bellerive, A. Review of Solar Neutrino Experiments. *Int. J. Mod. Phys. A* **2004**, *19*, 1167–1179. [CrossRef]
9. Mann, A.K. *Shadow of a Star: The Neutrino Story of Supernova 1987A*; W.H. Freeman and Co.: New York, NY, USA, 1997.
10. Barger, V.; Marfatia, D.; Whisnant, K.L. *The Physics of Neutrinos*; Princeton University Press: Princeton, NJ, USA, 2012.
11. Gonzalez-Garcia, M.C.; Maltoni, M.; Salvado, J.; Schwetz, T. Global Fit to Three Neutrino Mixing: Critical Look at Present Precision. *J. High Energ. Phys.* **2012**, *123*, 1–23. [CrossRef]
12. Planck Collaboration. *Planck* 2018 Results: VI. Cosmological Parameters. *Astron. Astrophys.* **2020**, *641*, A6. [CrossRef]
13. KATRIN Collaboration. Direct Neutrino-Mass Measurement Based on 259 Days of KATRIN Data. *Science* **2025**, *388*, 180–185. [CrossRef]
14. Esteban, I.; Gonzalez-Garcia, M.C.; Maltoni, M.; Martinez-Soler, I.; Pinheiro, J.P.; Schwetz, T. NuFit-6.0: Updated Global Analysis of Three-Flavor Neutrino Oscillations. *J. High Energ. Phys.* **2024**, *216*, 1–31. [CrossRef]
15. Kayser, B. 13. Neutrino Mass, Mixing, and Flavor Change. *Phys. Lett. B* **2008**, *667*, 163–171. [CrossRef]
16. Drewes, M. The Phenomenology of Right Handed Neutrinos. *Int. J. Mod. Phys. E* **2013**, *22*, 1330019–1330593. [CrossRef]
17. Boyarsky, A.; Drewes, M.; Lasserre, T.; Mertens, S.; Ruchayskiy, O. Sterile Neutrino Dark Matter. *Prog. Part. Nucl. Phys.* **2019**, *104*, 1–224. [CrossRef]
18. Ibe, M.; Kusenko, A.; Yanagida, T.T. Why Three Generations? *Phys. Lett. B* **2016**, *758*, 365–369. [CrossRef]
19. Aguilar-Arevalo, A.A.; Brown, B.C.; Bugel, L.; Cheng, G.; Conrad, J.M.; Cooper, R.L.; Dharmapalan, R.; Diaz, A.; Djurcic, Z.; Finley, D.A.; et al. Significant Excess of Electronlike Events in the MiniBooNE Short-Baseline Neutrino Experiment. *Phys. Rev. Lett.* **2018**, *121*, 221801. [CrossRef] [PubMed]
20. Abazajian, K.N. Sterile Neutrinos in Cosmology. *Phys. Rep.* **2017**, *711–712*, 1–28. [CrossRef]
21. Bryman, D.A.; Shrock, R. Constraints on Sterile Neutrinos in the MeV to GeV Mass Range. *Phys. Rev. D* **2019**, *100*, 073011. [CrossRef]
22. Hindi, M.M.; Avci, R.; Hussein, A.H.; Kozub, R.L.; Miočinović, P.; Zhu, L. Search for the Admixture of Heavy Neutrinos in the Recoil Spectra of ^{37}Ar Decay. *Phys. Rev. C* **1998**, *58*, 2512–2525. [CrossRef]
23. Smith, P.F. Proposed Experiments to Detect keV-Range Sterile Neutrinos Using Energy-Momentum Reconstruction of Beta Decay or K-Capture Events. *New J. Phys.* **2019**, *21*, 053022. [CrossRef]
24. Voytas, P.A.; Ternovan, C.; Galeazzi, M.; McCammon, D.; Kolata, J.J.; Santi, P.; Peterson, D.; Guimarães, V.; Becchetti, F.D.; Lee, M.Y.; et al. Direct Measurement of the L/K Ratio in ^{7}Be Electron Capture. *Phys. Rev. Lett.* **2002**, *88*, 012501. [CrossRef] [PubMed]
25. Friedrich, S.; Kim, G.B.; Bray, C.; Cantor, R.; Dilling, J.; Fretwell, S.; Hall, J.A.; Lennarz, A.; Lordi, V.; Machule, P.; et al. Limits on the Existence of Sub-MeV Sterile Neutrinos from the Decay of Be 7 in Superconducting Quantum Sensors. *Phys. Rev. Lett.* **2021**, *126*, 021803. [CrossRef] [PubMed]
26. Kim, I.; Bray, C.; Marino, A.; Stone-Whitehead, C.; Lamm, A.; Abells, R.; Amaro, P.; Andoche, A.; Cantor, R.; Diercks, D.; et al. Signal processing and spectral modeling for the BeEST experiment. *Phys. Rev. D* **2025**, *111*, 052010. [CrossRef]
27. Tilley, D.R.; Cheves, C.M.; Godwin, J.L.; Hale, G.M.; Hofmann, H.M.; Kelley, J.H.; Sheu, C.G.; Weller, A.H. Energy Levels of Light Nuclei A=5, 6, 7. *Nucl. Phys. A* **2002**, *708*, 3–163. [CrossRef]
28. Smolsky, J.; Leach, K.G.; Abells, R.; Amaro, P.; Andoche, A.; Borbridge, K.; Bray, C.; Cantor, R.; Diercks, D.; Fretwell, S.; et al. Direct experimental constraints on the spatial extent of a neutrino wavepacket. *Nature* **2025**, *638*, 640–644. [CrossRef] [PubMed]